Systematic Prioritisation of AI-Detected Chest X-ray Abnormalities for Optimised Lung Cancer Detection

Rhidian Bramley[1], Anna Sharman[2] Rebecca Duerden[3], Sarah Lyon[1], Melissa Ryan[4], Elodie Weber[5], Louise Brown[12], Matthew Evison[12]

[1]Greater Manchester Cancer Alliance, c/o The Christie NHS Foundation Trust, Manchester, UK; [2]Stockport NHS Foundation Trust, Stockport, UK; [3]Manchester University NHS Foundation Trust, Manchester, UK; [4]; Annalise.ai, Sydney NSW, Australia; [5] Sectra Imaging IT Solutions, Linköping, Sweden.

Corresponding author: Dr Rhidian Bramley. rhidian.bramley@nhs.net

1. ***Acknowledgements***

The authors wish to thank the Greater Manchester Cancer Alliance, the participating NHS Trusts, and Annalise.ai for their support in this study. We also acknowledge Sectra Imaging IT Solutions for providing the platform for deploying the AI system.

2. ***Funding***

This study has received funding from the NHS England National AI Diagnostic Fund (AIDF).

Compliance with Ethical Standards

3. ***Guarantor:***

The scientific guarantor of this publication is Dr Rhidian Bramley.

4. ***Conflict of Interest:***

The following authors of this manuscript declare relationships with the following companies:
Melissa Ryan: Annalise.ai, which provided the AI system used in this study.
Elodie Weber: Sectra Imaging IT Solutions, who provided the Amplifier platform and PACS

The other authors of this manuscript declare no relationships with any companies, whose products or services may be related to the subject matter of the article.

5. ***Statistics and Biometry:***

Melissa Ryan kindly provided statistical advice for this manuscript.

6. ***Informed Consent:***

Written informed consent was not required for this study because the study involved a service evaluation conducted in shadow mode with anonymised data, posing no impact on patient care.

7. ***Ethical Approval:***

The project was performed as part of a service evaluation project, so the Christie NHS Foundation Trust Research and Innovation Department and Quality Improvement and Clinical Audit Committee confirmed that Research Ethics approval was not required for this data analysis. All data used in this study were anonymised prior to analysis to ensure patient privacy. Data processing adhered to GDPR regulations and NHS information governance standards to maintain confidentiality.

8. ***Study subjects or cohorts overlap:***

Some study subjects or cohorts have been previously reported in the Greater Manchester Cancer Alliance diagnostic accuracy evaluations.

9. ***Methodology***

Methodology:

- Retrospective and observational study for cohort 1.
- Prospective and observational study for cohort 2.
- Multicentre study conducted across seven NHS Trusts in Greater Manchester.

Abstract

Objective: This study aimed to establish a reproducible method for selecting AI-detected chest X-ray (CXR) abnormalities prioritised for urgent reporting to support faster lung cancer diagnosis. By selecting findings informed by cancer prevalence and clinical significance, we sought to maximise detection while maintaining a high negative predictive value (NPV).

Materials and Methods: Two cohorts of CXRs were evaluated: (1) a retrospective cohort of patients with confirmed lung cancer and abnormal CXRs, and (2) a prospective cohort of primary care referred CXRs from seven Greater Manchester trusts, with the AI system in shadow mode. The AI triage system (Annalise Enterprise CXR) evaluated the relative prevalence of 124 abnormalities, and prioritisation strategies were assessed using sensitivity, specificity, positive predictive value (PPV), and NPV.

Results: A total of 1,282 lung cancer patients were included in cohort 1. In cohort 2, the AI system processed 13,802 CXRs. Sensitivity was 95.87% (94.77%-96.97%) in cohort 1, and specificity was 79.11% (78.43%-79.79%) in cohort 2, with an NPV of 99.95%.

Conclusion: This study presents a systematic, reproducible method for prioritising AI-detected CXR abnormalities, balancing high sensitivity and NPV while minimising low-risk prioritisation. This approach provides a data-driven alternative to traditional methods relying solely on clinical judgement.

Introduction

The rapid identification and prompt actioning of imaging, particularly chest x-rays (CXR) that suggest lung cancer, is crucial for improving patient outcomes and aligning with the National Optimal Lung Cancer Pathway[1] . For most patients, except those presenting with haemoptysis, the first diagnostic test for symptoms that could indicate lung cancer is a CXR [2]. These symptoms span a range of alternative diagnoses leading to an exceptionally high volume of CXR performed - over 8 million per year in England [3]. However, the incidence of lung cancer in CXR requested in primary care is just 1.4% [4]. This scenario creates substantial demand for CXR reporting in a context where radiology departments are stretched, with most CXR returning normal findings.

According to the 2023 Clinical Radiology Census Report, the NHS spent £276 million on outsourcing, insourcing and temporary locums to manage the overwhelming reporting demand, the highest expenditure on record [5]. The report also highlighted that this workforce shortages contribute to unacceptable diagnostic delays, including for patients undergoing CXR.

Artificial Intelligence (AI) has been proposed as one solution to these challenges. AI-driven tools can identify CXR findings suspicious for lung cancer and flag them for expedited reporting. Traditional approaches for AI-based prioritisation often rely heavily on clinical, focusing on a small subset of findings deemed significant. However, this method may be subjective and may not always reflect the true prevalence of AI detected abnormalities across patient cohorts.

This study addresses the need for a more systematic, evidence-based approach to identifying which CXR findings should guide AI prioritisation. The primary objective is to establish a rapid and reproducible method for selecting AI-detected CXR abnormalities for urgent reporting, supporting faster diagnosis of lung cancer. Here, we present an approach developed in Greater Manchester that enhances selection through empirical data rather than intuition alone. This study provides robust evidence to guide prioritisation, addressing an important gap in real-world AI implementation.

Methods

Study Setting and Population

The study was conducted across seven acute care trusts in Greater Manchester. Two distinct patient cohorts were evaluated with inclusion criteria for each cohort outlined below:

1. **Cohort 1**: A retrospective cohort of 1,282 patients with confirmed lung cancer and an abnormal CXR between 1st June 2020 and 1st June 2022. These cases were curated for a parallel diagnostic accuracy study. Patients were included if they had a CXR within six months of their lung cancer diagnosis, with the CXR report identifying an abnormality that required follow-up.
2. **Cohort 2**: A prospective analysis was designed to include all primary care CXRs, performed between 1st June 2024 and 30th July 2024, with the AI system running in shadow mode. All included CXRs were GP-referred, collected consecutively, and represented the general population undergoing CXR.

This study was conducted as a service evaluation under the governance of the participating trusts and did not require formal ethical approval. All data were anonymised prior to analysis in accordance with NHS information governance standards and GDPR regulations. The project complied with the UK Policy Framework for Health and Social Care Research.

Reference Standard

For cohort 1, every study was considered positive for lung cancer, owing to the definition of their inclusion criteria. For cohort 2, a 1% detectable lung cancer prevalence was assumed, in line with published studies and previous audits. The assumed prevalence alleviated the need for resource intensive ground truthing and accounted for the low prevalence finding in an otherwise normal cohort.

AI System

The **Annalise Container CXR (version 2.1; Annalise-AI)** was deployed using the Sectra Amplifier Platform. This AI system can detect up to 124 distinct findings on CXR, offering a comprehensive assessment of abnormalities During prospective data collection, the AI system was deployed in shadow mode, meaning that the outputs were not visible to clinical staff and did not influence patient care or diagnostic decisions. This ensured that the evaluation posed no risks to patient safety while allowing for a robust assessment of the system's performance. It analysed every CXR in both cohorts, generating an output for each of the 124 possible findings. The results were then anonymised and exported as comma-separated values (CSV) for further analysis.

Patients were not involved in the design or conduct of this study. As the study focused on evaluating the technical performance of AI in a shadow mode without direct patient impact, patient involvement was not deemed necessary.

Selection of Findings

An Excel-based tool was developed to evaluate the prevalence of AI-detected abnormalities across the two cohorts. The ratio of findings prevalence in cohort 1 compared to cohort 2 was computed as a metric to facilitate finding selection. The AI findings were classed into 3 initial priority groups through consensus by the supplier and clinical leads.

1. CRITICAL – Findings that potentially require urgent action. These were to be prioritised independent of whether they related to cancer.
2. HIGH – Findings of clinical significance that may need to be prioritised.
3. STANDARD – Other findings considered not to warrant clinical prioritisation.

Three prioritisation strategies for cancer were developed to determine which of the initial high priority group should be prioritised to optimise the detection of cancer:

1. **Strategy 1**: The 19 AI findings with the highest prevalence ratio (>5), maximising specificity.
2. **Strategy 2**: All the HIGH findings with a prevalence ratio greater than 2, enhancing sensitivity.
3. **Strategy 3**: A final set of findings based on clinical judgement, balancing sensitivity and specificity.

A clinical reference group, including thoracic radiologists and chest physicians, reviewed the findings' relative prevalence in both cohorts and refined the final set of findings for prioritisation.

Statistical Analysis

The performance of the AI system was evaluated by calculating sensitivity, specificity, positive predictive value (PPV), negative predictive value (NPV), false positive rate (FPR), and false negative rate (FNR) for each strategy. Sensitivity was determined using cohort 1 (lung cancer patients), while specificity, PPV, and NPV were estimated using cohort 2 (general referral population) . The Excel tool also calculated the number of CXRs needed to be reported to detect one cancer case to help set expectations for the AI's clinical impact.

In cohort 1, all chest X-rays (CXRs) were from 1,282 patients with confirmed lung cancer visible on CXR, providing a clear standard to calculate sensitivity:

$$Sensitivity = \frac{True\ Positives\ (TP)}{True\ Positives\ (TP) + False\ Negatives\ (FN)}$$

Equation 1

For cohort 2, a 1% detectable cancer prevalence was assumed based on published studies and previous audits of primary care CXRs, translating to an estimated 136 cancer positive cases in cohort 2 from a total 13,802 CXR. The True positives in this cohort were estimated as 136 x Sensitivity (computed from Cohort 1). The remaining cancer-negative cases (13,466) minus the false positives (FP) were used to calculate specificity:

$$Specificity = \frac{True\ Negatives\ (TN)}{True\ Negatives\ (TN) + False\ Positives\ (FP)}$$

Equation 2

Results

A total of 1,282 CXRs meeting the inclusion criteria were identified in cohort 1, and 13,802 CXRs meeting the inclusion criteria were included in cohort 2. Based on the assumed 1% lung cancer prevalence in cohort 2, this comprised 138 lung cancer positive cases and 13,664 lung cancer negative cases. The prevalence of all findings in each cohort and relative prevalences are shown in Supplementary Data (ST 1). The mean age in the cancer cohort was 71.4 years (SD ± 9.98), and the mean age in the referral cohort was 59.5 years (SD ± 17.4). There was no difference in the sex ratio between the cancer and referral cohorts, with 46.8% male and 53.2% female in each cohort. The flow of studies from each cohort is illustrated in Figure 1.

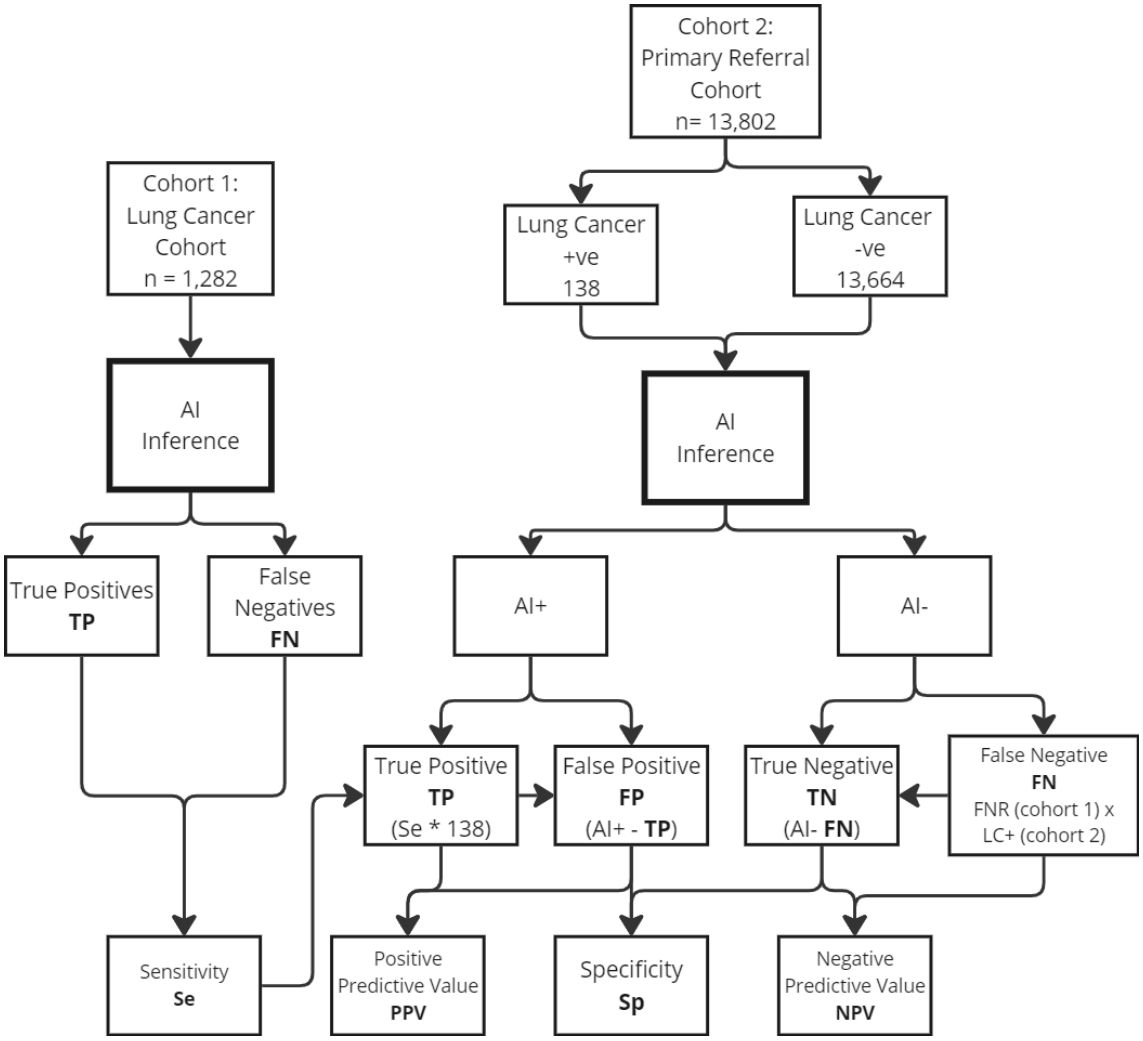

Figure 1: Flow diagram indicating inclusion of studies from each cohort, classification by the AI device and how the performance metrics were computed. The AI classifications varied based on the configuration of findings used.

The performance of the AI system across the three prioritisation strategies is summarised below and in Table 1:

Strategy	**Strategy 1 (>5 ratio)**	**Strategy 2 (All HIGH)**	**Strategy 3 (Clinical Review)**
AI Findings selected	19	41	32
Percent with AI finding (Cohort 1)	**13.59%**	**37.92%**	**21.64%**
Percent with AI finding (Cohort 2)	**92.82%**	**97.27%**	**95.87%**
True Positive (Cohort 1)	1190	1247	1229
False Negative (Cohort 1)	92	35	53
True Negative (Cohort 2)	11916	8564	10809
False Positive (Cohort 2)	1748	5100	2855
True Positive (Cohort 2)	128	134	132
False Negative (Cohort 2)	10	4	6
Sensitivity (95% CI)	92.82% (91.42% -94.25%)	97.27% (96.37% - 98.18%)	95.87% (94.77% - 96.97%)
Specificity (95% CI)	87.21% (86.65% - 87.77%)	62.68% (61.87% - 63.49%)	79.11% (78.43% - 79.79%)
Positive predictive value (PPV)	6.83%	2.56%	4.43%
Negative predictive value (NPV)	99.92%	99.96%	99.95%
False Positive Rate (FPR)	12.79%	37.32%	20.89%
False Negative Rate (FNR)	7.18%	2.73%	4.13%
AI Positive Cancer Detection rate (No CXR to report to detect 1 cancer)	15	39	23
AI Negative Cancer Detection rate (No CXR to report to detect 1 cancer)	1204	2274	1895

Table 1: Performance metrics of the AI system across three prioritisation strategies for chest X-ray findings, including sensitivity, specificity, positive predictive value (PPV), and negative predictive value (NPV). PPV: Positive predictive value – the proportion of AI-positive cases that are true positives. NPV: Negative predictive value – the proportion of AI-negative cases that are true negatives. FPR: False positive rate – the proportion of non-cancer cases flagged by AI. FNR: False negative rate – the proportion of cancer cases missed by AI.

Strategy 1: Prioritising the 19 AI findings classed as HIGH risk with a prevalence ratio greater than 5 for cancer resulted in a sensitivity of 92.82% and specificity of 87.21%. This strategy offered the highest specificity but at the expense of lower sensitivity.

Strategy 2: Including AI findings classed as HIGH risk with improved sensitivity to 97.27% but reduced specificity to 62.68%.

Strategy 3: The final set of findings, incorporating clinical judgement, resulted in a sensitivity of 95.87% in cohort 1, detecting 1,229 of the 1,282 patients with lung cancer. Specificity in cohort 2 was 79.11%, and the NPV was 99.95%.

Given that a small percentage of the referral population will have detectable cancer on a CXR, we conducted a statistical analysis to determine how specificity changes at cancer prevalence rates ranging from 0.5%, to 2% in the referral cohort. The results for each prioritisation strategy 3 incorporating clinical judgment under these prevalence scenarios ranges from 78.73% for a prevalence of 0.5% to 79.87% for a prevalence of 2%. This can be expressed as a confidence interval on the specificity based on the estimated cancer prevalence.

Discussion

This study presents a novel and reproducible approach to prioritising CXR AI findings, combining empirical data with clinical judgement to optimise diagnostic accuracy. We employed a two-cohort design to assess both the sensitivity and specificity of the AI system for lung cancer detection on chest X-rays, addressing the challenges of using real-world data in a low-caner prevalence setting. The cancer prevalence in patients referred from primary care according to NICE NG12 referral guideline in a large retrospective study was 1.4%[4]. The HealthCare Safety Investigation Branch has flagged that up to 20% of lung cancers are not detectable on CXR [6], so the number of detectable cancers is closer to 1% [7]

Calculating sensitivity required a retrospective cohort (cohort 1) with confirmed lung cancer cases, ensuring a sufficient number of verified positives to serve as the “ground truth”. This approach enabled a rigorous evaluation of the AI system’s ability to detect cancer in a cohort where all cases had a

confirmed diagnosis visible on CXR, eliminating the need to wait for sufficient cancer cases to present from the referral population.

For specificity, we used a prospective cohort (cohort 2) in which the AI was run for a brief period in shadow mode on primary care CXRs. This approach allowed us to calculate specificity and understand the AI's likely performance in identifying non-cancer cases within a referral population, thereby simulating the AI's real-world impact without clinical risk.

By combining retrospective sensitivity with prospective prevalence estimates, this study design offered a safe and practical means to inform prioritisation strategies. This two-cohort method provides a valuable framework for assessing AI diagnostic tools prior to live clinical implementation, particularly in areas where the prevalence of the condition in the referral population is low.

The findings with the highest prevalence ratio in the HIGH priority list included solitary lung mass, inferior mediastinal mass, diffuse upper airspace opacity, diffuse airspace opacity, cavitating mass with content, hilar lymphadenopathy, and multiple masses or nodules. Interestingly, many bone related abnormalities (e.g. kyphosis, osteopaenia, spinal arthritis, and diffuse spinal osteophytes) also exhibited a higher prevalence in the lung cancer cohort. This was attributed to the difference in patient age between the cohorts, the average age in the cancer cohort more than 10 years over the referral cohort. Whilst the prevalence of findings in each cohort provides general insights, the overall objective was to identify a list of findings that would maximise the detection of suspected lung cancer cases, while ensuring critical findings were prioritised, and avoiding the unnecessary prioritisation of low-risk cases (thereby maintaining a high NPV). This study demonstrates a systematic approach to selecting AI-detected CXR findings for prioritisation in the context of lung cancer diagnosis. By analysing the prevalence of 124 findings in both a lung cancer cohort and a general referral population, we developed a data-driven method that maximises sensitivity while maintaining a high NPV.

Strategy 1, which focused only on the findings with the highest prevalence ratio, achieved high specificity but had a lower sensitivity. **Strategy 2**, which included all non-critical findings that may warrant prioritisation achieved the highest sensitivity but lowest specificity for cancer. **Strategy 3**, which balanced statistical prevalence with clinical judgement, offered the optimal combination of sensitivity and specificity, achieving a sensitivity of 95.87% and an NPV of 99.95%.

While this approach effectively prioritised cases with a high likelihood of cancer, the impact on non-prioritised cases warrants further exploration. Delays in reporting less critical findings could potentially affect patient outcomes for non-cancer conditions. Future studies should evaluate how

prioritisation strategies impact overall diagnostic workflows and reporting times for all patients, including those with low-priority findings.

Strengths The approach proposed here differs from traditional methods by systematically prioritising findings based on their observed prevalence in cancer versus non-cancer cohorts, rather than relying solely on expert opinion. It is also reproducible across other ICBs implementing AI CXR prioritisation as part of the national AIDF programme. The methodology employed here can allow rapid completion of an initial study to support efficient implementation without the need for long term outcome data from prospective cohorts. The Excel workbook developed as part of this study was instrumental in refining our approach to AI finding prioritisation. By providing a platform to model different combinations of findings and instantly visualise their impact on diagnostic accuracy, this tool enabled a more data-driven and clinically relevant selection process. Future studies may benefit from adopting similar tools to streamline the integration of AI into clinical practice, particularly in settings where resource optimisation is critical.

Limitations. The prioritisation system was developed and tested using data cohorts from patients within the same region, which introduces a risk of overestimating clinical performance without external validation. Additionally, the selected findings may not generalise to different geographical areas or populations. External validation could be achieved by applying the tool to population cohorts outside Greater Manchester, which presents an opportunity for collaboration and further evaluation.

It is important to note that the performance metrics reported in this study are indicative rather than definitive. The reference standard for cohort 2 relies on an assumed prevalence, and analyses were conducted at the count level rather than validated against individual study-level reference standards. Consequently, some cases flagged as positive by the device may not be true positives, and some false positives could potentially represent true positives.

However, the primary aim of this study was not to determine the diagnostic accuracy of the device but to identify findings that optimise sensitivity and negative predictive value (NPV). Expanding the inclusion of clinically relevant findings and applying the methodology to additional referral populations is expected to influence positive and negative predictive values. Nonetheless, the main objective was to select findings that maximise sensitivity and NPV for identifying suspected lung cancer cases.

Future directions include validating the findings and prioritisation strategies in diverse patient populations and healthcare settings. A priority is to conduct multicentre prospective clinical implementation studies to evaluate real-world performance, including operational impacts on reporting workflows. Collaborations with imaging networks are planned to ensure broader generalisability and external validation of the methodology.

Although patients were not directly involved in the design of this study, future work will incorporate patient perspectives, particularly regarding the ethical implications of prioritisation strategies. Engaging patients in the development of communication strategies for AI prioritisation will enhance transparency and trust in these technologies.

Conclusion

Conclusion

This study presents a reproducible method for prioritising AI-detected CXR abnormalities, balancing the need for high sensitivity and NPV while accepting a lower PPV to avoid missing cancer cases and ensure early detection. By prioritising findings that maximise sensitivity, this approach improves the likelihood of identifying patients with suspected lung cancer. The use of shadow mode ensures clinical safety prior to full deployment, offering a practical, data-driven alternative to traditional judgement-based methods. With further validation, this approach could serve as a blueprint for integrating AI into radiology workflows, offering scalable solutions to global diagnostic challenges.

Key Points

Key Point 1 - Question

Explain the unmet need/clinical problem your study addresses (20-25 words)

What is the best way to systematically prioritise AI-detected chest X-ray abnormalities to support faster and more accurate lung cancer diagnosis?

Key Point 2 - Findings

Objectively summarize your main result (20-25 words)

This study demonstrated that prioritisation strategies can maximise sensitivity (95.87%) and negative predictive value (99.95%), while balancing specificity (79.11%) to ensure efficient lung cancer detection.

Key Point 3 - Clinically Relevant Statement

Summarize the benefit for the patient and/or clinical relevance of the study (max. 40 words)

By prioritising clinically significant findings, this methodology improves early lung cancer detection, enhances reporting workflows, and supports scalable AI integration into radiology, benefiting patients and healthcare systems.

Clinical Relevance Statement

The proposed prioritisation approach enhances early lung cancer detection by integrating AI into reporting workflows, addressing radiology demand and workforce constraints.

Keywords

- Lung cancer
- Chest X-ray
- Artificial intelligence
- Diagnostic prioritisation
- Radiology workflow

References

[1] NHS England, 'Implementing a Timed Lung Cancer Diagnostic Pathway'. Accessed: Oct. 27, 2024. [Online]. Available: https://www.england.nhs.uk/long-read/implementing-a-timed-lung-cancer-diagnostic-pathway/

[2] National Institute for Health and Care Excellence (NICE), 'Suspected cancer: recognition and referral', NG12: Lung and pleural cancers. Accessed: Oct. 27, 2024. [Online]. Available: https://www.nice.org.uk/guidance/ng12/chapter/Recommendations-organised-by-site-of-cancer#lung-and-pleural-cancers

[3] NHS England, 'Diagnostic Imaging Dataset 2023-24 Data'. Accessed: Oct. 27, 2024. [Online]. Available: https://www.england.nhs.uk/statistics/statistical-work-areas/diagnostic-imaging-dataset/diagnostic-imaging-dataset-2023-24-data/

[4] B. S. K. Bhartia *et al.*, 'The incidence of lung cancer amongst primary care chest radiograph referrals—an evaluation of national and local datasets within the United Kingdom', *British Journal of Radiology*, vol. 97, no. 1163, pp. 1769–1774, Nov. 2024, doi: 10.1093/bjr/tqae142.

[5] The Royal College of Radiologists, '2023 clinical radiology and clinical oncology workforce census reports'. Accessed: Oct. 27, 2024. [Online]. Available: https://www.rcr.ac.uk/news-policy/latest-updates/2023-clinical-radiology-and-clinical-oncology-workforce-census-reports/

[6] Healthcare Safety Investigation Branch, 'Missed detection of lung cancer on chest X-rays of patients being seen in primary care', HSIB Investigation report. Accessed: Oct. 27, 2024. [Online]. Available: https://www.hssib.org.uk/patient-safety-investigations/missed-detection-of-lung-cancer-on-chest-x-rays-of-patients-being-seen-in-primary-care/

[7] S. H. Bradley *et al.*, 'Estimating lung cancer risk from chest X-ray and symptoms: a prospective cohort study', *British Journal of General Practice*, vol. 71, no. 705, pp. e280–e286, Apr. 2021, doi: 10.3399/bjgp20X713993.

Supplementary material ESM

Supplementary Table 1 (ST1):

Initial Priority	AI Finding	Final priority	Count of studies (Cohort 1)	Count of studies (Cohort 2)	% of studies (cohort 1)	% of studies (cohort 2)	Prevalence Ratio (Cancer vs Referral)
Critical	Acute humerus fracture	P1	2	2	0.16%	0.01%	10.8
Critical	Acute clavicle fracture	P1	1	1	0.08%	0.01%	10.8
Critical	Widened aortic contour	P1	3	10	0.23%	0.07%	3.2
Critical	Simple pneumothorax	P1	6	34	0.47%	0.25%	1.9
Critical	Acute rib fracture	P1	17	228	1.33%	1.65%	0.8
Critical	Pneumomediastinum	P1	0	1	0.00%	0.01%	0.0
Critical	Tension pneumothorax	P1	0	4	0.00%	0.03%	0.0
Critical	Subdiaphragmatic gas	P1	0	4	0.00%	0.03%	0.0
Critical	Suboptimal ETT	P1	0	0	0.00%	0.00%	0.0
Critical	Suboptimal NGT	P1	0	0	0.00%	0.00%	0.0
Critical	Suboptimal CVC	P1	0	12	0.00%	0.09%	0.0
Critical	Scapular fracture	P1	0	2	0.00%	0.01%	0.0
Critical	Shoulder dislocation	P1	0	2	0.00%	0.01%	0.0
Critical	Suboptimal PAC	P1	0	0	0.00%	0.00%	0.0
Critical	Suboptimal gastric band	P1	0	2	0.00%	0.01%	0.0
Critical	Subcutaneous emphysema	P1	1	0	0.08%	0.00%	0.0
High	Solitary lung mass	P2	551	72	42.98%	0.52%	82.4
High	Inferior mediastinal mass	P2	91	18	7.10%	0.13%	54.4
High	Diffuse upper airspace opacity	P2	23	9	1.79%	0.07%	27.5
High	Diffuse airspace opacity	P2	9	4	0.70%	0.03%	24.2
High	Cavitating mass with content	P2	30	14	2.34%	0.10%	23.1
High	Spinal wedge fracture	P2	18	9	1.40%	0.07%	21.5
High	Hilar lymphadenopathy	P2	139	74	10.84%	0.54%	20.2
High	Multiple masses or nodules	P2	160	87	12.48%	0.63%	19.8
High	Perihilar airspace opacity	P2	13	8	1.01%	0.06%	17.5
High	Lung collapse	P2	12	8	0.94%	0.06%	16.1
High	Cavitating mass(es)	P2	64	53	4.99%	0.38%	13.0
High	Diffuse lower airspace opacity	P2	54	55	4.21%	0.40%	10.6
High	Solitary lung nodule	P2	411	474	32.06%	3.43%	9.3
High	Segmental collapse	P2	181	210	14.12%	1.52%	9.3
High	Loculated effusion	P2	31	39	2.42%	0.28%	8.6
High	Focal airspace opacity	P2	639	825	49.84%	5.98%	8.3
High	Multifocal airspace opacity	P2	104	144	8.11%	1.04%	7.8
High	Spinal lesion	P2	1	2	0.08%	0.01%	5.4
High	Pleural mass	P2	37	83	2.89%	0.60%	4.8
High	Superior mediastinal mass	P2	56	131	4.37%	0.95%	4.6
High	Diffuse pleural thickening	P2	15	37	1.17%	0.27%	4.4
High	Upper interstitial thickening	P2	195	508	15.21%	3.68%	4.1
High	Upper zone fibrotic volume loss	P2	53	157	4.13%	1.14%	3.6
High	Rib lesion	P2	39	122	3.04%	0.88%	3.4
High	Simple effusion	P2	289	953	22.54%	6.90%	3.3
High	Diffuse nodular / miliary lesions	P2	20	68	1.56%	0.49%	3.2
High	Lower zone fibrotic volume loss	P2	24	89	1.87%	0.64%	2.9
High	Tracheal deviation	P2	75	285	5.85%	2.06%	2.8
High	Diffuse interstitial thickening	P2	57	292	4.45%	2.12%	2.1
High	Scapular lesion	P2	2	12	0.16%	0.09%	1.8
High	Humeral lesion	P2	6	51	0.47%	0.37%	1.3
High	Internal foreign body	P2	1	38	0.08%	0.28%	0.3
High	Clavicle lesion	P2	0	9	0.00%	0.07%	0.0
High	Calcified mass (> 5mm)	P3	23	126	1.79%	0.91%	2.0
High	Pulmonary artery enlargement	P3	13	79	1.01%	0.57%	1.8
High	Basal interstitial thickening	P3	169	1042	13.18%	7.55%	1.7
High	Distended bowel	P3	5	50	0.39%	0.36%	1.1
High	Widened cardiac silhouette	P3	170	2080	13.26%	15.07%	0.9
High	Diffuse fibrotic volume loss	P3	2	41	0.16%	0.30%	0.5
High	Pulmonary congestion	P3	16	333	1.25%	2.41%	0.5
High	Peribronchial cuffing	P3	26	814	2.03%	5.90%	0.3
Standard	Kyphosis	P3	23	6	1.79%	0.04%	41.3
Standard	Osteopaenia	P3	21	8	1.64%	0.06%	28.3
Standard	Spinal arthritis	P3	42	18	3.28%	0.13%	25.1

Standard	Diffuse spinal osteophytes	P3	4	2	0.31%	0.01%	21.5
Standard	Post resection volume loss	P3	19	60	1.48%	0.43%	3.4
Standard	Lower zone bullae	P3	5	16	0.39%	0.12%	3.4
Standard	Upper zone bullae	P3	27	88	2.11%	0.64%	3.3
Standard	Rib resection	P3	3	12	0.23%	0.09%	2.7
Standard	Reduced lung markings	P3	45	191	3.51%	1.38%	2.5
Standard	Aortic stent	P3	2	10	0.16%	0.07%	2.2
Standard	Diffuse bullae	P3	1	5	0.08%	0.04%	2.2
Standard	Aortic arch calcification	P3	539	3016	42.04%	21.85%	1.9
Standard	Gallstones	P3	3	17	0.23%	0.12%	1.9
Standard	Calcified hilar lymphadenopathy	P3	3	17	0.23%	0.12%	1.9
Standard	Hyperinflation	P3	318	1938	24.80%	14.04%	1.8
Standard	Mastectomy	P3	25	158	1.95%	1.14%	1.7
Standard	Coronary stent	P3	9	59	0.70%	0.43%	1.6
Standard	Incompletely imaged chest	P3	108	717	8.42%	5.19%	1.6
Standard	Calcified pleural plaques	P3	34	226	2.65%	1.64%	1.6
Standard	Diaphragmatic elevation	P3	138	950	10.76%	6.88%	1.6
Standard	Calcified axillary nodes	P3	5	35	0.39%	0.25%	1.5
Standard	Shoulder replacement	P3	7	50	0.55%	0.36%	1.5
Standard	Mediastinal clips	P3	42	305	3.28%	2.21%	1.5
Standard	Axillary clips	P3	21	169	1.64%	1.22%	1.3
Standard	Patient rotation	P3	305	2509	23.79%	18.18%	1.3
Standard	Bronchiectasis	P3	25	209	1.95%	1.51%	1.3
Standard	Hiatus hernia	P3	34	298	2.65%	2.16%	1.2
Standard	Lung sutures	P3	4	37	0.31%	0.27%	1.2
Standard	Atelectasis	P3	162	1529	12.64%	11.08%	1.1
Standard	Electronic cardiac devices	P3	29	274	2.26%	1.99%	1.1
Standard	Calcified granuloma (< 5mm)	P3	24	235	1.87%	1.70%	1.1
Standard	Chronic rib fracture	P3	48	474	3.74%	3.43%	1.1
Standard	Unfolded aorta	P3	321	3333	25.04%	24.15%	1.0
Standard	Scoliosis	P3	74	810	5.77%	5.87%	1.0
Standard	Chronic humerus fracture	P3	5	56	0.39%	0.41%	1.0
Standard	Rotator cuff anchor	P3	7	81	0.55%	0.59%	0.9
Standard	Sternotomy wires	P3	30	349	2.34%	2.53%	0.9
Standard	Gastric band	P3	1	12	0.08%	0.09%	0.9
Standard	Diaphragmatic eventration	P3	107	1310	8.35%	9.49%	0.9
Standard	Breast implant	P3	5	62	0.39%	0.45%	0.9
Standard	Nipple shadow	P3	24	301	1.87%	2.18%	0.9
Standard	Chronic clavicle fracture	P3	8	102	0.62%	0.74%	0.8
Standard	Shoulder fixation	P3	2	26	0.16%	0.19%	0.8
Standard	Underexposed	P3	2	30	0.16%	0.22%	0.7
Standard	Abdominal clips	P3	23	368	1.79%	2.67%	0.7
Standard	Cervical flexion	P3	5	80	0.39%	0.58%	0.7
Standard	Neck clips	P3	4	65	0.31%	0.47%	0.7
Standard	Shoulder arthritis	P3	5	82	0.39%	0.59%	0.7
Standard	Spinal fixation	P3	2	35	0.16%	0.25%	0.6
Standard	Pericardial fat pad	P3	11	368	0.86%	2.67%	0.3
Standard	Cardiac valve prosthesis	P3	2	88	0.16%	0.64%	0.2
Standard	Underinflation	P3	1	90	0.08%	0.65%	0.1
Standard	Airway stent	P3	0	1	0.00%	0.01%	0.0
Standard	Clavicle fixation	P3	0	17	0.00%	0.12%	0.0
Standard	Calcified neck nodes	P3	0	13	0.00%	0.09%	0.0
Standard	Image obscured	P3	0	0	0.00%	0.00%	0.0
Standard	Intercostal drain	P3	0	0	0.00%	0.00%	0.0
Standard	In position CVC	P3	0	18	0.00%	0.13%	0.0
Standard	In position NGT	P3	0	0	0.00%	0.00%	0.0
Standard	In position ETT	P3	0	0	0.00%	0.00%	0.0
Standard	Biliary stent	P3	0	3	0.00%	0.02%	0.0
Standard	Oesophageal stent	P3	0	1	0.00%	0.01%	0.0
Standard	In position PAC	P3	0	0	0.00%	0.00%	0.0
Standard	Rib fixation	P3	0	2	0.00%	0.01%	0.0
Standard	Pectus excavatum	P3	0	2	0.00%	0.01%	0.0
Standard	Overexposed	P3	0	0	0.00%	0.00%	0.0
Standard	Pectus carinatum	P3	0	0	0.00%	0.00%	0.0
No Findings	NULL - no findings	P3	4	3350	0.31%	24.27%	0.0